SCIENCE CHINA Materials

ARTICLES

mater.scichina.com link.springer.com

Published online 6 September 2017 | doi: 10.1007/s40843-017-9086-9

Sci China Mater 2017, 60(9): 849–856

Defective MoS_2 electrocatalyst for highly efficient hydrogen evolution through a simple ball-milling method

Li-Fang Zhang[1,2], Xiaoxing Ke[3], Gang Ou[2], Hehe Wei[2], Lu-Ning Wang[1*] and Hui Wu[2*]

ABSTRACT **Molybdenum disulfide (MoS_2) has attracted extensive attention as an alternative to replace noble electrocatalysts in the hydrogen evolution reaction (HER). Here, we highlight an efficient and straightforward ball milling method, using nanoscale Cu powders as reductant to reduce MoS_2 engineering S-vacancies into MoS_2 surfaces, to fabricate a defect-rich MoS_2 material (DR-MoS_2). The micron-sized DR-MoS_2 catalysts exhibit significantly enhanced catalytic activity for HER with an overpotential (at 10 mA cm^{-2}) of 176 mV in acidic media and 189 mV in basic media, surpassing most of Mo-based catalysts previously reported, especially in basic solution. Meanwhile stability tests confirm the outstanding durability of DR-MoS_2 catalysts in both acid and basic electrolytes. This work not only opens a new pathway to implant defects to MoS_2, but also provides low-cost alternative for efficient electrocatalytic production of hydrogen in both alkaline and acidic environments.**

Keywords: electrocatalyst, hydrogen evolution, MoS_2, defects, S-vacancies

INTRODUCTION

Hydrogen has been vigorously pursued as a future clean and renewable energy carrier in the transition from the current hydrocarbon economy, due to the fossil fuels consumption. Particularly, sustainable hydrogen producing in terms of water splitting has attracted growing attention [1]. Electrochemically splitting water into hydrogen is one of most convenient and promising method among various energy storage techniques [2,3]. A number of devices for water electrolysis are designed to function in acidic electrolyte, in which the state-of-the-art hydrogen evolution reaction (HER) catalysts are most based on noble metal such as Pt [4–6]. However, the high price and scarcity of the noble metal have critically impeded the large-scale application for hydrogen energy [7]. Thus it still remains a challenge to develop highly active HER catalysts based on materials that are more abundant at lower cost [8–14].

Molybdenum disulfide (MoS_2), an earth-abundant and high activity material, has attracted extensive attention as an alternative to replace noble electrocatalysts in the HER [15–18]. MoS_2 has a hexagonally layered packed structure, consisting of a single layer of Mo between two sulfur layers in a trigonal prismatic arrangement. These cumulate sandwiched S–Mo–S layers are held together by van der Waals force and piled in a graphite-like structure to form bulk material [19]. Up to now, many efforts have been made to improve the performance of MoS_2 as HER catalysts [20–24]. There are two strategies to optimize the electrochemical performance of MoS_2 including revealing active sites and increasing the electrical conduction for improving the electron transfer [25,26]. Introducing defects has proven to be an effective approach to generate active sites [27]. During the past few years, previous studies confirm that the HER activity of MoS_2 correlates with the number of catalytically active edge sites. Hence, efforts have been made to focus on developing MoS_2 electrocatalysts with abundant active edge sites [28,29]. Wang *et al.* [30] reported ultrasmall molybdenum sulfide nanoparticles with the enrichment of S edges on molybdenum sulfide, showing extremely high catalytic efficiency. Xie *et al.* [31] developed a scalable pathway to accomplish the task of engineering defects onto MoS_2 surfaces to expose active edge sites, showing superior HER electrocatalytic activity. However, few approaches

[1] School of Materials Science and Engineering, University of Science and Technology Beijing, Beijing 100083, China
[2] School of Materials Science and Engineering, Tsinghua University, Beijing 100084, China
[3] Institute of Microstructure and Property of Advanced Materials, Beijing University of Technology, Beijing 100124, China
[*] Corresponding authors (emails: luning.wang@ustb.edu.cn (Wang LN); huiwu@tsinghua.edu.cn (Wu H))

have sought to make use of the basal plane, which constitutes the majority of the bulk material. Very recently, several studies reported that the basal plane of MoS_2 was successfully activated by creating sulphur (S)-vacancies. S-vacancies introduce gap states that are favorable to hydrogen adsorption [32,33]. Zheng *et al.* [34] reported that the monolayer 2H-MoS_2 by introducing S-vacancies and straining yielded an optimal hydrogen adsorption free energy (ΔG_H) equivalent to 0 eV, achieving the highest intrinsic HER activity among molybdenum-sulfide-based catalysts. Jin *et al.* [35] suggested that both edges and S-vacancies also contribute significantly to the catalytic activity in porous MoS_2. Despite the enormous strides and many achievements we have made, practical use of MoS_2 electrocatalysts is still hampered by some limitations: the short lifetime of electrode materials, low catalytic activity especially in alkaline-based condition, and the complex fabrication process [36,37].

Herein, we highlight an efficient and straightforward ball milling method, using nanoscale Cu powders as reductant to reduce MoS_2 engineering S-vacancies into MoS_2 surfaces, to fabricate a defect-rich MoS_2 material (DR-MoS_2). The ball milling method, a costly-effective and efficient approach for scale-up production, in which the strong shear forces are generated between high-speed rotating balls not only produces small-scaled materials but also promotes the reaction with Cu and orginal MoS_2, introducing rich active sites *via* the formation of defects within the material. The as-formed DR-MoS_2 catalysts exhibit significantly enhanced catalytic activity for HER with an overpotential (at 10 mA cm^{-2}) of 176 mV in acidic media and 189 mV in basic media, surpassing most of Mo-based catalysts previously reported, especially in basic solution. Meanwhile stability tests confirm the outstanding durability of DR-MoS_2 catalysts in both acid and basic electrolytes.

EXPERIMENTAL SECTION

Preparation of the DR-MoS_2 materials

The DR-MoS_2 catalysts were prepared by a one-step ball milling method. Commercially-available MoS_2 powders (99.9%) and excess nanoscaled Cu powders were dissolved in ethanol solution and then placed in a grinding bowl flushed with argon. After ball milling for 24 h at 700 rpm, the precipitate was collected by centrifugation and washed with nitric acid, distilled water and ethanol repeatedly for eight times to remove residue Cu and orther intermediates. The precipitate was dried at 70°C overnight and ground for further experiments. For comparison, MoS_2 (named BM-MoS_2) with the same quality was also ball milled by the same procedure but without the addition of nanoscaled Cu.

Electrochemical measurements

All electrochemical measurements were carried out using a CHI 660E electrochemical workstation. A three-electrode system was adopted to evaluate the electrochemical performance with a graphite rod as the counter electrode and Ag/AgCl (in saturated KCl solution) electrode as reference electrode. The catalyst was ultrasonically dispersed in a water-ethanol solution (v/v=3:1) containing 0.1 wt.% Nafion to form a homogeneous ink. Then the mixed ink were attached onto a glass carbon (GC) electrode with 4 mm diameter (loading 2.8 mg cm^{-2}) as working electrode, polished with alumina slurry and cleaned with ethanol and distilled (DI) water before loading. Linear-sweep voltammetry (LSV) measurements were conducted in 0.5 mol L^{-1} H_2SO_4 and 1.0 mol L^{-1} KOH at scan rates from 5 to 300 mV s^{-1}. The stability tests for the catalysts were performed with the time dependent current density measurement, where a constant overpotential was 220 mV *vs.* reversible hydrogen electrode (RHE) both in 0.5 mol L^{-1} H_2SO_4 and 1.0 mol L^{-1} KOH. All of the potentials were referenced to a RHE.

Characterization

The morphology of the prepared samples was investigated by scanning electron microscopy (SEM, MERLIN VP Compact, Carl Zeiss, Germany) and transmission electron microscopy (TEM, FEI Titan G2) operated at 300 kV. Images were acquired at low dose in order to minimize beam damage. X-ray diffraction (XRD) patterns were obtained by using a D/max-2500 diffractometer with a Cu Kα irradiation source (λ = 1.54 Å). X-ray photoelectron spectroscopy (XPS) spectra were obtained with an ESCALAB 250Xi from Thermo Fisher Scientific electron spectrometer using an Al Kα radiation. The particle size of samples was measured by laser scattering particle analyzer (Hydro 2000NW, MAlver, Worcestershire, UK). Photoluminescence (PL) spectra and Raman spectra were measured on a microscopic confocal Raman spectrometer (Raman, LabRAM HR800, HORIBA Jobin Yvon, Villeneuve d'Ascq, France) using a 514 nm laser as the excitation source.

RESULTS AND DISCUSSION

The DR-MoS_2 catalysts were prepared by a one-step ball milling method. The as-formed DR-MoS_2 catalysts have a well-defined layer structure as shown in Fig. 1a and the

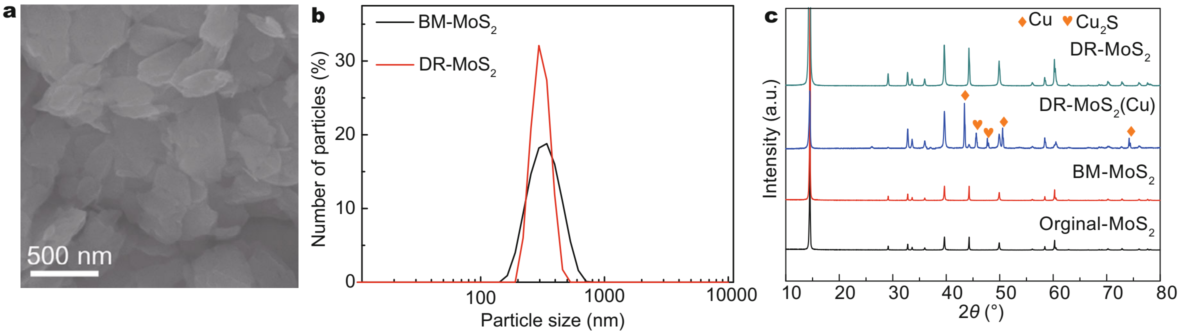

Figure 1 (a) SEM image shows the morphology of the DR-MoS_2 powders; (b) particle size analysis of the DR-MoS_2 and BM-MoS_2; (c) XRD patterns of different samples. DR-MoS_2 (Cu) is the ball-milled MoS_2 without Cu removal. Cu_2S and residue Cu are clearly observed after ball milling, indicating the reaction between Cu and MoS_2.

majority of the particles are in the range of 50–500 nm, quite consistent with the particle size analysis result (Fig. 1b). The average particle size of DR-MoS_2 is 443 nm, almost same with the ball-milled MoS_2 without the addition of Cu (BM-MoS_2). XRD were carried out to further investigate the phase information of the product. As shown in Fig. 1c, all diffraction peaks of the DR-MoS_2 catalysts agree well with the original MoS_2, revealing the high purity of the product. The presence of Cu_2S peak in the product without being washed [DR-MoS_2 (Cu)] demonstrates a reduction of MoS_2 by Cu.

Defects induced during ball milling would lead to strains. It is thus useful to study the sample at nanoscale to evaluate the strains locally. The DR-MoS_2 and BM-MoS_2 were then studied by high resolution TEM (HRTEM) as shown in Fig. 2. Fig. 2a is the HTREM image where the area of BM-MoS_2 was indicated by arrows. Geometric phase analysis (GPA) was performed and corresponding strain components were shown in Fig. 2b–d. The color scale was included in the figure, which shows different strain components quantitatively. For comparison, the HRTEM of BM-MoS_2 at the same imaging condition is shown in Fig. 2e, with the corresponding strain components (Fig. 2f–h) plotted using the same color scale. It is clear that the BM-MoS_2 is nearly defect-free, whereas the DR-MoS_2 presents significantly higher amount of strain and thus defects.

Raman and PL spectra were also applied to investigate the difference of DR-MoS_2 and BM-MoS_2. As shown in Fig. 3a, the peak position of DR-MoS_2 shifts from 401.51 to 402.53 cm^{-1} for A_{1g} mode (the out-of-plane optical vibration mode of S atoms), and from 374.23 to 376.07 cm^{-1} for E^1_{2g} mode (the in-plane optical vibration mode of Mo-S bond). Consequently, the position of A_{1g} mode blue shifts about 1.02 cm^{-1}, while E^1_{2g} mode blue shifts about 1.84 cm^{-1}. The Raman spectra confirms lattice distortion [38]. Furthermore, intensity of the DR-MoS_2 PL peak (680 nm) also decreases compared to BM-MoS_2, as shown in Fig. 3b. Thus, the decrease of PL intensity further suggests that more defects and cracks are formed on DR-MoS_2. Overall, the changes of the Raman and PL spectra suggest that during the ball milling process, sulfur atoms are effectively removed from the intact specimen and the defects are generated, which may benefit for MoS_2 as an electrochemical catalyst. XPS was further used to confirm the formation of S-vacancies in the DR-MoS_2 sample. It is clearly observed that the doublet signals corresponding to S-2$p_{1/2}$ and S-2$p_{3/2}$ of DR-MoS_2 shift towards low binding energy comparing to BM-MoS_2, demonstrating that the number of S atom decreased and S-vacancies were generated (Fig. 3c) [34]. Furthermore, Mo^{4+} 3$d_{3/2}$ and 3$d_{5/2}$ signals of DR-MoS_2 are observed around 233 and 230 eV, respectively, almost same with BM-MoS_2, confirming the original structure of MoS_2 is still remained (Fig. 3d).

HER activity of the samples was analyzed using a conventional three-electrode setup with 0.5 mol L^{-1} H_2SO_4 as electrolyte. All curves presented here were corrected for the voltage drop due to solution resistivity (IR drop), measured before each run *via* electrochemical impedance spectroscopy (EIS). As shown in Fig. 4a, the overpotential of DR-MoS_2, 176 mV at the current density of 10 mA cm^{-2}, is more positive than that of BM-MoS_2, suggesting a prominent HER activity. From the extrapolation of the linear region of overpotential (η) *versus* log$j$ (Fig. 4b), we obtained Tafel slopes of 22, 63, and 85 mV per decade for Pt/C, DR-MoS_2, and BM-MoS_2, respectively. The Tafel slope of DR-MoS_2 falls within the range of 40–120 mV dec^{-1}, indicating that the HER would proceed through a Volmer-Heyrovsky mechanism, and

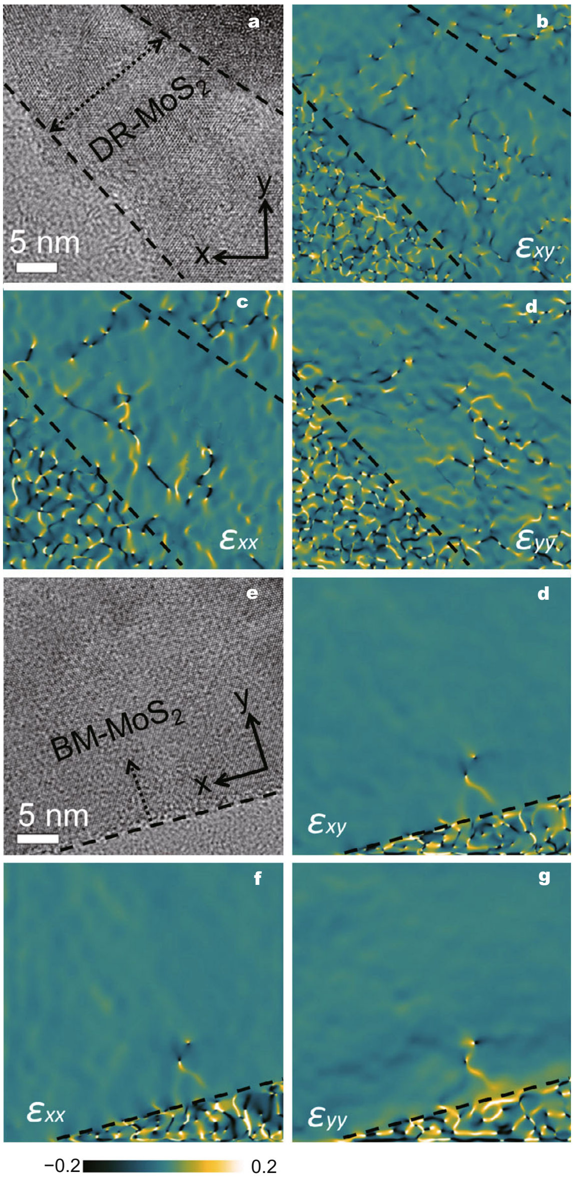

Figure 2 HRTEM image (a) and the corresponding strain maps (b–d) of DR-MoS_2: the area of DR-MoS_2 is confined by the dash lines in (a). The corresponding strain maps are shown in (b–d), which reveals the presence of strains in the specimen. HRTEM image (e) and the corresponding strain maps (f–g) of BM-MoS_2: the area of BM-MoS_2 is indicated by an arrow. The corresponding strain maps are shown in (f–g), indicating that the specimen is almost defect-free. Color scale is shown at the bottom of the figure.

the desorption of hydrogen is the rate limiting step. From the intercept of the linear region of the Tafel plots, the exchange current density is determined to be 7.6 μA cm^{-2} for the DR-MoS_2 sample, almost one order of magnitude higher than that of BM-MoS_2 (0.50 μA cm^{-2}), again suggesting the excellent HER catalytic activity. Durability of catalysts should be one of the most important aspects for their real applications. To investigate the electrochemical stability of DR-MoS_2 catalysts, we carried out a long-term test in acid electrolytes. Obviously, as shown in Fig. 4c, after 24 h the DR-MoS_2 catalysts exhibit negligible degradation, revealing the superior stability in an acid environment. We list a number of latest literature about Mo-based materials and compare their HER performance in acidic condition in Fig. 4d. It can be noticed that the low overpotential of DR-MoS_2 (176 mV *vs.* RHE for achieving 10 mA cm^{-2}) is better than or at least comparable to most of the reported Mo-based HER catalysts.

We further investigated the HER performance of the DR-MoS_2 in 1.0 mol L^{-1} KOH. As shown in Fig. 5a, the polarization curve recorded for the DR-MoS_2 exhibits a lower overpotential at j = 10 mA cm^{-2} in basic media, 189 mV at j = 10 mA cm^{-2}. The fitted Tafel plot of the DR-MoS_2 in Fig. 5b gives a Tafel slop value of 98 mV dec^{-1}, which is much lower than that of BM-MoS_2. The exchange current densities (j_0) for DR-MoS_2 is 0.063 mA cm^{-2}, which outperforms that of BM-MoS_2 (0.031 mA cm^{-2}). Potentiostatic test was performed to assess the electrochemical stability of the DR-MoS_2 electrode in an basic environment. As shown in Fig. 5c, the current density stabilized up to 24 h while the DR-MoS_2 electrode performed still steadily, suggested by the smooth curve recorded after 24 h along with negligible current degradation.

It should be noted that Mo-based catalysts available in the literature usually perform relatively lower HER activity in basic media because of the limited amount of hydrogen ions for proton reduction reaction in basic solution. Only several examples of Mo-based catalysts have been tested for HER in basic media. Our DR-MoS_2 catalysts only required 189 mV to achieve 10 mA cm^{-2}, showing better performance than most HER catalysts in basic solution (Fig. 5d). Thus, this work represented a new breakthrough for advanced MoS_2 electrocatalysts highly performed in a basic media for HER.

During the ball milling process, the reaction between Cu and MoS_2 occurs, and thus sulfur atoms are removed effectively from the surface and S-vacancies are created. According to previous studies, S-vacancies introduce gap states that allow favorable hydrogen adsorption. Increasing the number of S-vacancy sites strengthens hydrogen adsorption, allowing the simultaneous manipulation of the hydrogen adsorption free energy ($\triangle G_H$) and the active site density. Therefore, the enhanced catalytic activity of DR-MoS_2 catalysts is mainly attributed to the S-vacancies.

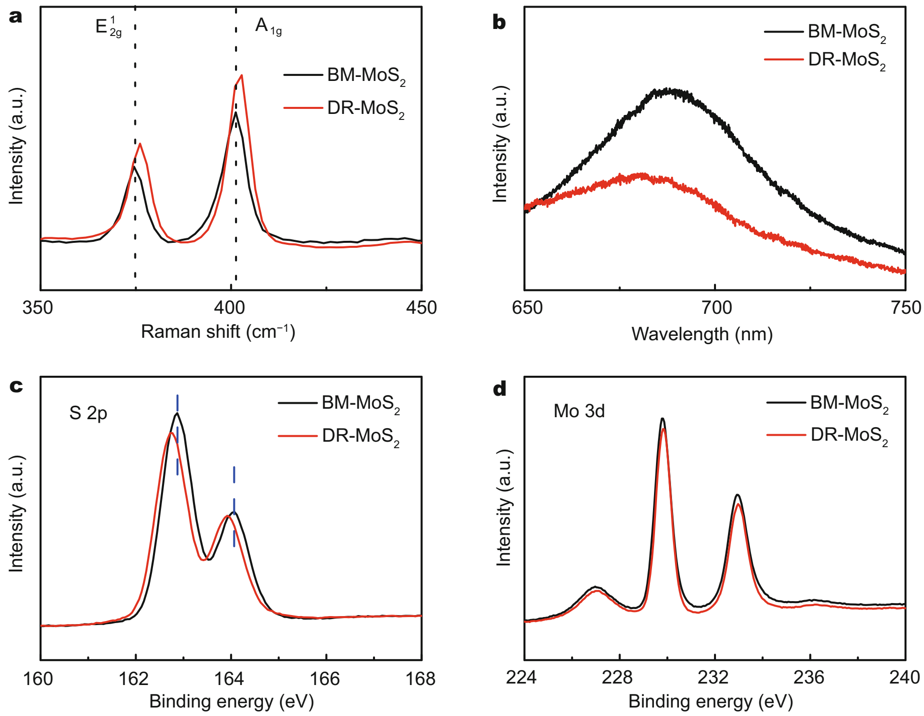

Figure 3 (a) Raman spectra of DR-MoS_2 and BM- MoS_2; (b) PL spectra of DR-MoS_2 and BM- MoS_2; XPS spectra of DR-MoS_2 and BM- MoS_2: (c) S 2p and (d) Mo 3d.

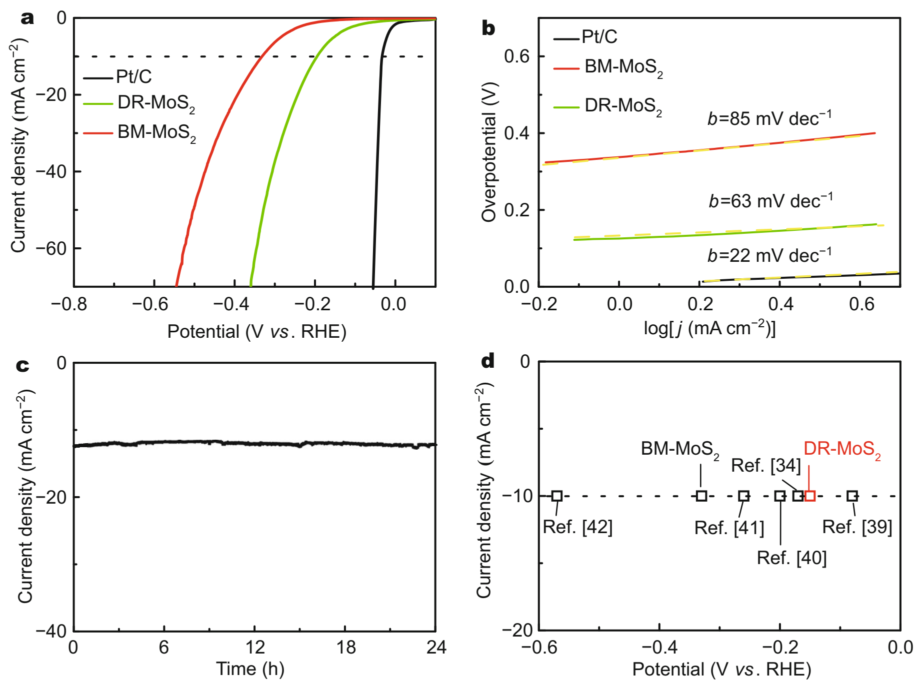

Figure 4 (a) HER polarization curves of various catalysts (Pt/C, DR-MoS_2 and BM- MoS_2) with a scan rate of 50 mV s^{-1} in 0.5 mol L^{-1} H_2SO_4; the comparison of overpotential for these catalysts were all measured at current density, 10 mA cm^{-2}; (b) the corresponding Tafel plots of various catalysts (Pt/C, DR-MoS_2 and BM- MoS_2). Yellow dashed line is the fitting slope of the corresponding Tafel plot. (c) The *I-t* curves of the DR-MoS_2 in 0.5 mol L^{-1} H_2SO_4. Test performed at 220 mV RHE. (d) Comparison of HER current density at 10 mA cm^{-2} *versus* overpotential for catalysts in acidic media. Catalysts include DR-MoS_2, BM-MoS_2 and others previously reported [34,39–42].

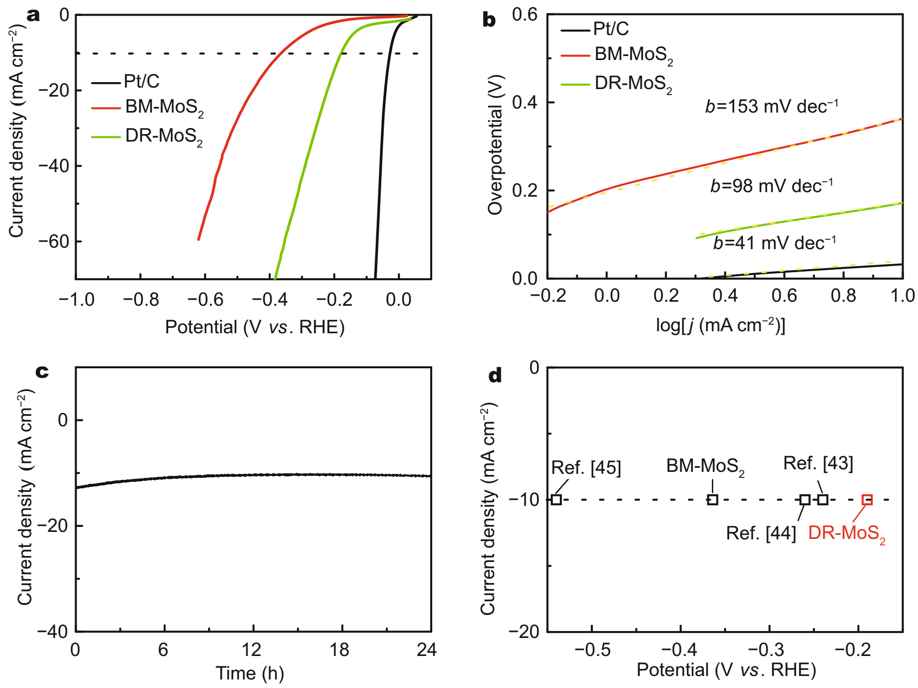

Figure 5 (a) The HER polarization curves of various catalysts (Pt/C, DR-MoS_2 and BM-MoS_2) with a scan rate of 50 mV s^{-1} in 1 mol L^{-1} KOH; the comparison of overpotential for these catalysts were all measured at current density, 10 mA cm^{-2}; (b) the corresponding Tafel plots of various catalysts (Pt/C, DR-MoS_2 and BM- MoS_2). Yellow dashed line is the fitting slope of the corresponding Tafel plot; (c) the *I-t* curves of DR-MoS_2 in 1 mol L^{-1} KOH; test performed at 220 mV RHE. (d) The HER current density at 10 mA cm^{-2} *versus* overpotential for various catalysts in basic media. Catalysts include DR-MoS_2, BM-MoS_2 and others previously reported [43–45].

CONCLUSION

In summary, we developed a simple ball-milling reducing method to fabricate a defect-enriched MoS_2 (DR-MoS_2) catalyst, showing excellent HER activity both in acid and basic media. The DR-MoS_2 catalysts exhibit significantly enhanced catalytic activity for HER with an overpotential (both tested at 10 mA cm^{-2}) of 176 mV in acid media and 189 mV in basic media, surpassing most of Mo-based catalysts previously reported, especially in basic solution. This study provides new and comprehensive insights to reveal the critical factors that influence the catalytic activity of MoS_2, which will enable the design and improvement of earth-abundant electrocatalysts based on MoS_2 and other layered materials with further enhanced catalytic performance.

Received 11 June 2017; accepted 1 August 2017; published online 6 September 2017

1 Chen HM, Chen CK, Liu RS, *et al.* Nano-architecture and material designs for water splitting photoelectrodes. Chem Soc Rev, 2012, 41: 5654–5671
2 Zou X, Zhang Y. Noble metal-free hydrogen evolution catalysts for water splitting. Chem Soc Rev, 2015, 44: 5148–5180
3 Lu S, Zhuang Z. Electrocatalysts for hydrogen oxidation and evolution reactions. Sci China Mater, 2016, 59: 217–238
4 Jiao Y, Zheng Y, Jaroniec M, *et al.* Design of electrocatalysts for oxygen- and hydrogen-involving energy conversion reactions. Chem Soc Rev, 2015, 44: 2060–2086
5 Stamenkovic VR, Mun BS, Arenz M, *et al.* Trends in electrocatalysis on extended and nanoscale Pt-bimetallic alloy surfaces. Nat Mater, 2007, 6: 241–247
6 Yang H, Wang C, Hu F, *et al.* Atomic-scale Pt clusters decorated on porous α-$Ni(OH)_2$ nanowires as highly efficient electrocatalyst for hydrogen evolution reaction. Sci China Mater, 2017, doi: 10.1007/s40843-017-9035-8
7 Morales-Guio CG, Stern LA, Hu X. Nanostructured hydrotreating catalysts for electrochemical hydrogen evolution. Chem Soc Rev, 2014, 43: 6555–6569
8 Chen WF, Sasaki K, Ma C, *et al.* Hydrogen-evolution catalysts based on non-noble metal nickel-molybdenum nitride nanosheets. Angew Chem Int Ed, 2012, 51: 6131–6135
9 Lu Q, Hutchings GS, Yu W, *et al.* Highly porous non-precious bimetallic electrocatalysts for efficient hydrogen evolution. Nat Commun, 2015, 6: 6567–6574
10 Xu X, Chen Y, Zhou W, *et al.* A perovskite electrocatalyst for efficient hydrogen evolution reaction. Adv Mater, 2016, 28: 6442–6448
11 Chen P, Xu K, Tao S, *et al.* Phase-transformation engineering in cobalt diselenide realizing enhanced catalytic activity for hydrogen evolution in an alkaline medium. Adv Mater, 2016, 28: 7527–7532
12 Xing Z, Liu Q, Asiri AM, *et al.* Closely interconnected network of molybdenum phosphide nanoparticles: a highly efficient electro-

catalyst for generating hydrogen from water. Adv Mater, 2014, 26: 5702–5707
13 Tang C, Cheng N, Pu Z, *et al.* NiSe nanowire film supported on nickel foam: an efficient and stable 3D bifunctional electrode for full water splitting. Angew Chem Int Ed, 2015, 54: 9351–9355
14 Yang Y, Xu X, Wang X. Synthesis of Mo-based nanostructures from organic-inorganic hybrid with enhanced electrochemical for water splitting. Sci China Mater, 2015, 58: 775–784
15 Zeng M, Li Y. Recent advances in heterogeneous electrocatalysts for the hydrogen evolution reaction. J Mater Chem A, 2015, 3: 14942–14962
16 Ge X, Chen L, Zhang L, *et al.* Nanoporous metal enhanced catalytic activities of amorphous molybdenum sulfide for high-efficiency hydrogen production. Adv Mater, 2014, 26: 3100–3104
17 Ji Q, Zhang Y, Shi J, *et al.* Morphological engineering of CVD-grown transition metal dichalcogenides for efficient electrochemical hydrogen evolution. Adv Mater, 2016, 28: 6207–6212
18 Yang X, Li Q, Hu G, *et al.* Controlled synthesis of high-quality crystals of monolayer MoS_2 for nanoelectronic device application. Sci China Mater, 2016, 59: 182–190
19 Chhowalla M, Shin HS, Eda G, *et al.* The chemistry of two-dimensional layered transition metal dichalcogenide nanosheets. Nat Chem, 2013, 5: 263–275
20 Hinnemann B, Moses PG, Bonde J, *et al.* Biomimetic hydrogen evolution: MoS_2 nanoparticles as catalyst for hydrogen evolution. J Am Chem Soc, 2005, 127: 5308–5309
21 Chen Z, Cummins D, Reinecke BN, *et al.* Core–shell MoO_3–MoS_2 nanowires for hydrogen evolution: a functional design for electrocatalytic materials. Nano Lett, 2011, 11: 4168–4175
22 Lu Q, Yu Y, Ma Q, *et al.* 2D transition-metal-dichalcogenide-nanosheet-based composites for photocatalytic and electrocatalytic hydrogen evolution reactions. Adv Mater, 2016, 28: 1917–1933
23 Liu S, Zhang X, Zhang J, *et al.* MoS_2 with tunable surface structure directed by thiophene adsorption toward HDS and HER. Sci China Mater, 2016, 59: 1051–1061
24 Liu J, Cao H, Jiang B, *et al.* Newborn 2D materials for flexible energy conversion and storage. Sci China Mater, 2016, 59: 459–474
25 Zhou W, Zou X, Najmaei S, *et al.* Intrinsic structural defects in monolayer molybdenum disulfide. Nano Lett, 2013, 13: 2615–2622
26 Liao L, Zhu J, Bian X, *et al.* MoS_2 formed on mesoporous graphene as a highly active catalyst for hydrogen evolution. Adv Funct Mater, 2013, 23: 5326–5333
27 Ouyang Y, Ling C, Chen Q, *et al.* Activating inert basal planes of MoS_2 for hydrogen evolution reaction through the formation of different intrinsic defects. Chem Mater, 2016, 28: 4390–4396
28 Wang H, Tsai C, Kong D, *et al.* Transition-metal doped edge sites in vertically aligned MoS_2 catalysts for enhanced hydrogen evolution. Nano Res, 2015, 8: 566–575
29 Kong D, Wang H, Cha JJ, *et al.* Synthesis of MoS_2 and $MoSe_2$ films with vertically aligned layers. Nano Lett, 2013, 13: 1341–1347
30 Wang T, Liu L, Zhu Z, *et al.* Enhanced electrocatalytic activity for hydrogen evolution reaction from self-assembled monodispersed molybdenum sulfidenanoparticles on an Au electrode. Energ Environ Sci, 2013, 6: 625–633
31 Xie J, Zhang H, Li S, *et al.* Defect-rich MoS_2 ultrathin nanosheets with additional active edge sites for enhanced electrocatalytic hydrogen evolution. Adv Mater, 2013, 25: 5807–5813
32 Ataca C, Ciraci S. Dissociation of H_2O at the vacancies of single-layer MoS_2. Phys Rev B, 2012, 85: 195410
33 Li H, Du M, Mleczko MJ, *et al.* Kinetic study of hydrogen evolution reaction over strained MoS_2 with sulfur vacancies using scanning electrochemical microscopy. J Am Chem Soc, 2016, 138: 5123–5129
34 Li H, Tsai C, Koh AL, *et al.* Activating and optimizing MoS_2 basal planes for hydrogen evolution through the formation of strained sulphur vacancies. Nat Mater, 2016, 15: 48–53
35 Lukowski MA, Daniel AS, Meng F, *et al.* Enhanced hydrogen evolution catalysis from chemically exfoliated metallic MoS_2 nanosheets. J Am Chem Soc, 2013, 135: 10274–10277
36 Merki D, Hu X. Recent developments of molybdenum and tungsten sulfides as hydrogen evolution catalysts. Energ Environ Sci, 2011, 4: 3878–3888
37 Staszak-Jirkovský J, Malliakas CD, Lopes PP, *et al.* Design of active and stable Co–Mo–Sx chalcogels as pH-universal catalysts for the hydrogen evolution reaction. Nat Mater, 2016, 15: 197–203
38 Kang N, Paudel HP, Leuenberger MN, *et al.* Photoluminescence quenching in single-layer MoS_2 *via* oxygen plasma treatment. J Phys Chem C, 2014, 118: 21258–21263
39 Ye TN, Lv LB, Xu M, *et al.* Hierarchical carbon nanopapers coupled with ultrathin MoS_2 nanosheets: highly efficient large-area electrodes for hydrogen evolution. Nano Energ, 2015, 15: 335–342
40 Kiriya D, Lobaccaro P, Nyein HYY, *et al.* General thermal texturization process of MoS_2 for efficient electrocatalytic hydrogen evolution reaction. Nano Lett, 2016, 16: 4047–4053
41 Benck JD, Chen Z, Kuritzky LY, *et al.* Amorphous molybdenum sulfide catalysts for electrochemical hydrogen production: insights into the origin of their catalytic activity. ACS Catal, 2012, 2: 1916–1923
42 Kibsgaard J, Chen Z, Reinecke BN, *et al.* Engineering the surface structure of MoS_2 to preferentially expose active edge sites for electrocatalysis. Nat Mater, 2012, 11: 963–969
43 Vrubel H, Hu X. Molybdenum boride and carbide catalyze hydrogen evolution in both acidic and basic solutions. Angew Chem, 2012, 124: 12875–12878
44 Zou X, Huang X, Goswami A, *et al.* Cobalt-embedded nitrogen-rich carbon nanotubes efficiently catalyze hydrogen evolution reaction at all pH values. Angew Chem, 2014, 126: 4461–4465
45 Merki D, Fierro S, Vrubel H, *et al.* Amorphous molybdenum sulfide films as catalysts for electrochemical hydrogen production in water. Chem Sci, 2011, 2: 1262–1267

Acknowledgements This work was supported by the National Basic Research of China (2015CB932500 and 2013CB632702) and the National Natural Science Fundation of China (51302141, 51501008, U1560103 and 61274015).

Author contributions Zhang LF performed the main experiments and analyzed the data with support from Ke X, Ou G, and Wei H. Zhang LF and Ke X wrote this manuscript. Wang LN and Wu H directly guided and conducted this work including the design, modifying and polishing. All authors contributed to the general discussion.

Conflict of interest The authors declare that they have no conflict of interest.

Supplementary information Experimental details and supporting data are available in the online version of the paper.

Li-Fang Zhang is now a PhD candidate of the School of Materials Science and Engineering, University of Science and Technology Beijing. Her current research is focused on the electrocatalysis for hydrogen evolution.

Lu-Ning Wang is a professor at the School of Materials Science and Engineering, University of Science and Technology Beijing. His research interests cover electrochemical process of functional materials and electrochemical process of materials in severe cultures.

Hui Wu received his BE degree in 2004 and PhD degree in 2009 from Tsinghua University. After postdoc. research in Prof. Yi Cui's group at Stanford University (2009–2013), he became an associate professor at the School of Materials Science and Engineering in Tsinghua University. He has received academic honors and awards including the 1000 Talents Program for Young Scholars, the National Outstanding Doctoral Dissertation Award, the Chief Youth Scientist of National 973 Program, the National Natural Science Funds for Outstanding Young Scholar and TR35. His research interest focuses on the materials for energy storage and conversion, advanced functional ceramic materials, flexible electronics materials.

球磨法制备富含缺陷的高性能二硫化钼析氢反应电催化剂

张丽芳[1,2], 柯小行[3], 欧刚[2], 魏呵呵[2], 王鲁宁[1*], 伍晖[2*]

摘要 通过电催化将水分解可大量制备高纯度氢气, 这一过程需要高效能低成本的电催化剂材料. 二硫化钼价格低廉、资源丰富, 且具有类似贵金属铂的氢吸附自由能, 是一种潜在的高效制氢电催化剂. 然而其仍面临着析氢过电位偏高、稳定性差、难以批量制备、在碱性环境下催化析氢活性较低等问题, 限制了其实际应用. 目前, 大量文献证实制造缺陷是一种有效的优化二硫化钼电催化活性的方法. 本文通过球磨还原法制备了一种富含缺陷的二硫化钼析氢反应电催化剂. 这种新型的富缺陷二硫化钼催化剂在酸碱性条件下都显示出较高的催化活性, 在酸性条件下, 过电位为176 mV时其电流密度可达10 mA cm^{-2}; 在碱性条件下, 过电位为189 mV时其电流密度可达10 mA cm^{-2}, 超过了大部分报道的析氢反应电催化剂. 此外, 富缺陷二硫化钼材料显示出较小的塔菲尔斜率和良好的电化学稳定性, 进一步证实了析氢反应催化活性的增强. 这种通过球磨还原制造缺陷的思路为未来催化剂的设计与性能优化开辟了一条新的道路, 且该方法简单, 适于大规模的工业生产.